NRL Memorandum Report 5136

Numerical and Analytical Studies of Beam Channel Tracking

AD A139148

B. HUI AND M. LAMPE

Plasma Theory Branch
Plasma Physics Division

February 29, 1984

This research was sponsored by the Defense Advanced Research Projects Agency (DoD) under ARPA Order No. 4395, Amendment No. 9, and monitored by the Naval Surface Weapons Center.

NAVAL RESEARCH LABORATORY
Washington, D.C.

DTIC ELECTE MAR 20 1984 S D
A

DTIC FILE COPY

Approved for public release; distribution unlimited.

84 03 20 044

SECURITY CLASSIFICATION OF THIS PAGE

REPORT DOCUMENTATION PAGE

1a. REPORT SECURITY CLASSIFICATION UNCLASSIFIED	1b. RESTRICTIVE MARKINGS
2a. SECURITY CLASSIFICATION AUTHORITY	3. DISTRIBUTION/AVAILABILITY OF REPORT Approved for public release; distribution unlimited.
2b. DECLASSIFICATION/DOWNGRADING SCHEDULE	
4. PERFORMING ORGANIZATION REPORT NUMBER(S) NRL Memorandum Report 5136	5. MONITORING ORGANIZATION REPORT NUMBER(S)
6a. NAME OF PERFORMING ORGANIZATION Naval Research Laboratory 6b. OFFICE SYMBOL (If applicable)	7a. NAME OF MONITORING ORGANIZATION Naval Surface Weapons Center
6c. ADDRESS (City, State and ZIP Code) Washington, DC 20375	7b. ADDRESS (City, State and ZIP Code) Silver Spring, MD 20910
8a. NAME OF FUNDING/SPONSORING ORGANIZATION DARPA 8b. OFFICE SYMBOL (If applicable)	9. PROCUREMENT INSTRUMENT IDENTIFICATION NUMBER
8c. ADDRESS (City, State and ZIP Code) Arlington, VA 22209	10. SOURCE OF FUNDING NOS. PROGRAM ELEMENT NO. 62707E; PROJECT NO.; TASK NO.; WORK UNIT NO. 47-0900-0-3
11. TITLE (Include Security Classification) NUMERICAL AND ANALYTICAL STUDIES OF BEAM CHANNEL TRACKING	
12. PERSONAL AUTHOR(S) B. Hui and M. Lampe	
13a. TYPE OF REPORT Interim 13b. TIME COVERED FROM 10/1/82 TO 10/1/83	14. DATE OF REPORT (Yr., Mo., Day) February 29, 1984 15. PAGE COUNT 42
16. SUPPLEMENTARY NOTATION This research was sponsored by the Defense Advanced Research Projects Agency (DoD) under ARPA Order No. 4395, Amendment No. 9, and monitored by the Naval Surface Weapons Center.	
17. COSATI CODES FIELD / GROUP / SUB. GR.	18. SUBJECT TERMS (Continue on reverse if necessary and identify by block number) Relativistic electron beam tracking; Electron beam plasma interaction; Electron beam propagation

19. ABSTRACT (Continue on reverse if necessary and identify by block number)

The interaction force between a rigidly displaced relativistic electron beam and a preformed channel is analyzed. The displacement is not assumed to be small. It is found that two types of equilibria can exist, either on axis with respect to the channel or displaced from the channel by a prescribed amount. The location of the equilibrium depends on the ratio of beam radius to channel radius and the types of channels.

20. DISTRIBUTION/AVAILABILITY OF ABSTRACT UNCLASSIFIED/UNLIMITED ☒ SAME AS RPT. ☐ DTIC USERS ☐	21. ABSTRACT SECURITY CLASSIFICATION UNCLASSIFIED
22a. NAME OF RESPONSIBLE INDIVIDUAL B. Hui	22b. TELEPHONE NUMBER (Include Area Code) (202) 767-3720 22c. OFFICE SYMBOL Code 4792

DD FORM 1473, 83 APR EDITION OF 1 JAN 73 IS OBSOLETE.

SECURITY CLASSIFICATION OF THIS PAGE

CONTENTS

I. INTRODUCTION 1

II. NUMERICAL RESULTS 6

III. ANALYTIC AND MODEL CALCULATIONS 12

IV. CONCLUSIONS 21

ACKNOWLEDGMENTS 22

REFERENCES 39

NUMERICAL AND ANALYTICAL STUDIES OF BEAM CHANNEL TRACKING

I. Introduction

An intense relativistic charged particle beam may be injected into a pre-formed channel in a neutral gas. The channel may have been formed in a variety of ways, i.e., with a laser, an electrical discharge, or a previous particle beam, and it may be simply a heated reduced-density region in pressure balance with the surrounding neutral gas (a density channel), or it may be ionized (a conductivity channel), or both. If the beam is displaced from the axis of the channel, the question arises as to whether electromagnetic forces are generated which tend to restore the beam to the channel axis or push it further away. We shall refer to these as channel tracking or detracking forces, respectively.

In this paper, we report on theoretical calculations of channel tracking phenomena for the case where there is no pre-existing current flowing in the channel. In this situation, the question of whether the beam will stay in the channel separates into three distinct problems. The first of these relates to the forces between the beam and the channel. If the pre-existing channel conductivity $\sigma(r)$ is not too high ($4\pi\sigma r_b \lesssim c$, where r_b is the beam radius and c is the speed of light), then electrostatic forces are slightly dominant in the front of the beam, back to about the pinch point[1]. Since electrostatic image forces are predominately attractive, one might expect the front of the beam to be attracted toward the channel. However, the actual situation turns out to be more complicated than one might expect, because of the peculiar properties of spatially-extended image charges. The near-cancellation of electrostatic and magnetic forces on a relativistic beam, and the interplay between pre-existing gas conductivity and beam-produced conductivity also

Manuscript approved December 19, 1983.

complicate matters. We shall refer to these questions as the tracking problem, proper. This alone is the subject of this paper.

In the main part of the beam, well behind the pinch point, the gas conductivity is large enough to insure space charge neutrality, and thus magnetic forces predominate. The force between the beam and the oppositely-directed plasma current in the channel is repulsive, and generally much stronger than the forces on the beam head. Nonetheless, the beam is not necessarily pushed out of the channel, because there are magnetic coupling forces that attract the beam toward the beam axis established by the head, which is itself attracted toward the channel (under some circumstances). The question of whether these beam-beam forces are strong enough to balance the repulsive beam-channel forces and permit an equilibrium to exist will be referred to as the self-coupling problem. The equilibrium, if it exists, may be such that the displacement of the beam axis from the channel axis increases with $\zeta \equiv ct - z$, the distance behind the beam head. This will be considered in a subsequent paper.

Assuming that an equilibrium exists, the question remains as to its stability properties, particularly to the hose instability. This stability problem has been studied at great length[2], but only in regard to a beam in a uniform medium, or a beam whose equilibrium is assumed to be on-axis in a channel. It is well-known that the presence of plasma return current is a destabilizing factor. However, stability properties remain a subject for future study, as regards the correct beam equilibria in the presence of a density or conductivity channel.

In this study, we consider a wide range of possible channel states. For specificity, the gas is taken to be air at 1 atm outside the channel, with on-axis channel density ranging from 0.1 atm to 1 atm, and a simple model for

ionization by the beam is included in the calculation. Within our model, the channel density affects the forces on the beam only indirectly, by means of the density-dependence of avalanche ionization and recombination, which in turn affect the conductivity of the gas. The pre-existing channel conductivity is varied from zero to a large value. The channel density is assumed to be independent of time and of the axial position z; the initial conductivity is also independent of z, but σ does depend on ζ due to beam-produced ionization. Our model also assumes that the initial $\sigma(r,\zeta)$ is axisymmetric about the original channel axis. The radial profiles of the initial channel density and conductivity are assumed to be Bennett.

In a real experiment, the ratio of the beam radius r_b to channel radius r_c varies quite a lot from the head of the beam to the tail. Near the head, the beam has a trumpet shape[1], so its radius may be much larger than the channel radius. Near the tail, the beam is well pinched so its radius can be smaller than the channel radius. Ideally one should use a self-consistent envelope equation for the beam radius but we have not incorporated that in our model at this point. We have adopted a simpler approach, which is to use a uniform pencil beam and study the dependence of tracking force on the ratio of r_b/r_c. Occasionally, we do assign an envelope shape to the beam, but this envelope is not coupled back to the fields; therefore, we should look at those results as only qualitative.

Throughout each run the beam is modeled as a rigid straight rod which may be displaced from the channel axis by a uniform time-independent displacement Y. We emphasize that we do <u>not</u> assume that Y is small. The geometry is shown in Fig. 1. Because neither the beam nor the channel are allowed to respond dynamically, we can calculate unambiguously the tracking force between the beam and the preformed channel. If the beam were allowed to bend, the

resultant force acting on the beam would have an additional component due to the coupling force between beam slices. This force is typically at least two orders of magnitude larger than the electrostatic tracking force and therefore the delicate physics of beam channel tracking can easily be overwhelmed. The adoption of a time independent approach also allows us to eliminate the hose motion (instability) which does not concern us in this report.

The numerical study is performed using the DYNASTY II[3] code developed at NRL. It solves Lee's ultrarelativistic approximation to the Maxwell field equations[4],

$$\nabla_\perp^2 A_z = -\frac{4\pi}{c} J_b - \sigma \frac{\partial}{\partial \zeta}(A_z - \phi), \tag{1a}$$

$$\nabla_\perp^2 \frac{\partial}{\partial \zeta}(A_z - \phi) = \nabla_\perp \cdot \frac{4\pi\sigma}{c} \nabla_\perp \phi, \tag{1b}$$

where A_z is the axial component of the vector potential, ϕ is the scaler potential, and σ is the gas conductivity, together with an air conductivity model that includes direct ionization, avalanche and recombination,

$$\frac{\partial}{\partial \zeta}\sigma(r,\zeta) = \kappa J_b(r) + (\alpha_E/c)\sigma - \beta_r \sigma^2. \tag{2}$$

Here $\kappa = 8.8\text{x}10^{-4}$ cm/statcoul, $\beta_r = 7.1\text{x}10^{-15}(\rho_g/\rho_o)$sec/cm, the avalanche coefficient α_E is a function of the ratio of the electric field E to the gas density ρ_g, given as Eqs. (17) and (18) of Ref. 5, and ρ_o is the air density at 1 atm. DYNASTY II is <u>not</u> linearized about cylindrical symmetry, as are

typical monopole/dipole beam codes[6,7]; therefore, we are not restricted to study only small beam displacement as required by linearized codes. This capability has allowed us to discover a new beam-channel equilibrium which was not observed before. To elucidate our rather surprising numerical results, we have also analyzed a solvable two-dimensional electrostatic tracking model which yields similar conclusions about the beam equilibria with respect to the channel. The stability and propagation characteristics with respect to these equilibria are unknown at this point.

To summarize our main results, we find that the beam head always tracks the channel provided the preformed channel conductivity $\sigma_o (= 4\pi\sigma r_b/c)$ is not bigger than 0.8 and not much smaller than 0.1. For a pencil beam, the equilibrium position of the beam head can be on or off the channel axis depending on the ratio of the width of the beam and the channel. A pure density channel results in a beam equilibrium off-axis in the channel for all cases studied. The body of the beam behind the pinch point[1] always feels a detracking force, and therefore will stay in the channel only if the self-coupling force holds it to the head. The electrostatic tracking force is very weak-- as much as five orders of magnitude weaker than the pinch force at full current, for typical cases studied with rise-time for the current in the range 30 r_b/c to 60 r_b/c. For typical laboratory experiments[8,9], this force is too small to be detected.

Section II discusses the numerical results; Section III describes the analytical calculations; and Section IV presents the conclusions.

II. Numerical Results

In this section, we present numerical results for the dependence of the tracking force on the beam radius, channel radius, channel pressure, channel conductivity, and current rise time. The geometry of the system is shown in Fig. 1 where the preformed channel is displaced as a rigid rod from the beam axis by an amount $\hat{e}_y$. The force on a slice of the beam at ζ is given by

$$F_t(\zeta) = K_o \int d^2\underset{\sim}{r}\, J_b(\zeta)\, \nabla_\perp [A_z(\zeta) - \phi(\zeta)] \cdot \hat{e}_y , \qquad (4)$$

where J_b is the beam current density. The beam and the channel profiles are chosen to be Bennett. K_o is a normalization constant, chosen to normalize the tracking force to the pinch force F_p of a beam at full current. We fix the beam radius to be $r_b = 0.5$ cm for pencil beams. The channel radius is varied from $0.5r_b$ to $1.5r_b$. All lengths (ζ and r_c) are normalized to r_b, and conductivity is expressed in the dimensionless units $4\pi\sigma r_b/c$. The maximum beam current is $I_{bo} = 10$ kA and it ramps up in ζ according to

$$I_b = I_{bo} [1 - \exp -(\zeta/\zeta_r)^2], \qquad (5)$$

where $\zeta \equiv ct - z$ is a measure of the distance along the axis from the beam head.

We have checked out the numerical validity of the code in the following ways. For $Y \ll 1$, we compare the results with the NRL linearized code SIMM1[7], and find the forces calculated by the two codes differ by only a few percent. For $Y \gtrsim 1$, we alternately displace the beam and the channel by the same Y to make sure they give the same result (within a few percent error). As an additional check, we displace both the beam and the channel together by the

same Y and we find the force (which should be zero) is typically less than one percent compared to when just the channel is displaced.

We shall use the following abbreviations to label the channels:

σ channel $\equiv$ a pure conductivity channel,

n channel $\equiv$ a pure density channel,

σ + n channel $\equiv$ a combination of conductivity and density channel.

The first set of runs are for pencil beams, i.e., r_b constant. Typical ζ-dependences of beam current density J_b on the beam axis, plasma current density J_p on the channel axis, axial electric field E_z on the channel axis, and conductivity σ on the channel axis near the beam head are shown in Fig. 2. Figures 3-6 show the dependence of the tracking force $F_t(\zeta)$, normalized to pinch force F_p at full current, on the channel radius r_c and displacement Y. Figure 3 shows plots for $r_c = 2.0$ and $Y = 0.1$. The σ and σ + n channels show tracking while the n channel does not. The peak tracking force for the σ and σ + n channels are about the same. These findings are in agreement with previous calculations that were linearized by assuming $Y \ll r_b$ and $Y \ll r_c$[10]. The σ channel initially has $\sigma_o = 0.1$ on axis and the n channel has density 0.1 atm on axis. If the displacement is increased to $Y = 1.5$, while keeping $r_c = 2.0$ (Fig. 4), the n channel now shows relatively good tracking (about ten times stronger than the σ channel with $Y = 0.1$). The tracking force for the σ and σ + n channels is even stronger, by another order of magnitude. Figures 3 and 4 show that σ and σ + n channels allow the beam to track on axis, with the tracking force stronger for a σ + n channel than for any other channel type, while the beam in an n channel feels a tracking force only when it is off axis. This off-axis tracking implies that the beam head is in unstable equilibrium when it is propagating slightly off axis in a

channel, but that an equilibrium exists with the beam head off-axis by a prescribed amount. Moreover, the equilibrium value of Y is an increasing function of ζ. It should be emphasized that these results cannot be obtained with linearized codes because these codes are restricted to values of $Y \ll 1$.

Figure 5 shows similar tracking force plots for $r_c = 0.5$. These results should give us an indication of how well the beam tracks near the blown-up head region. We find that the beam feels a detracking force in any type of channel for values of Y up to 1.0 (curves a-c). For larger displacement, Y = 1.5, the force is reversed and tracking occurs (curves d-f). These results suggest that the blown-up beam head will never propagate coaxially with the preformed channels, but can reach an equilibrium position off axis. Whether this will drive hose instability remains to be determined.

In Fig. 6, we show the dependence of the tracking force as a function of displacement Y at a fixed value of $\zeta = 9.0$, for a case with $r_c = 0.5r_b$. This clearly indicates that the beam is unstable to small displacement, but that at larger Y, the beam polarizes the channel and the force becomes attractive. Consequently, for $r_c/r_b < 1.0$, the beam head will sit somewhere off axis with respect to the channel.

The cases for $r_c = 1.0$ are shown in Fig. 7. This situation resembles the neck region of the beam. Again we find for all types of channels that the beam detracks for small Y and tracks for larger Y, with the $\sigma + n$ channel giving the strongest tracking. Notice that in contrast to the case with $r_c = 0.5$ (Fig. 5), the case Y = 1.0 now gives some tracking. This indicates the larger the channel radius, the easier it is for the beam to track the channel. This point is illustrated in Fig. 8 where we compare the tracking force for cases with $r_c = 2.0$ and 5.0, with Y = 0.1 in both cases. The case with $r_c = 5.0$

gives a much stronger tracking force and its tracking region in ζ is twice as long.

The dependence of the tracking force on the current rise time ζ_r (measured in units of ζ) is shown in Fig. 9. A longer current rise time essentially "stretches" the tracking region in ζ and weakens the peak tracking force, but it does not change the sign of the tracking force.

For all the cases presented in Fig. 3-9, beam-channel forces become detracking at larger ζ. This is to be expected because in the magnetic regime (where the gas conductivity is high and the beam space charge is neutralized), the repulsive magnetic force between the beam and the return current dominates. This does not mean that part of the beam is repelled and breaks away from the beam head. Once the beam head tracks the channel, the self-coupling force is usually strong enough to hold the rest of the beam together provided the initial conductivity is not too large. The dynamical response of a beam to various types of channels in the linearized regime has been studied by Masamitsu, et al.[10].

There exists a critical conductivity $\sigma_o = \sigma_c$ above which the beam never tracks the channels for any values of r_c and Y. For $\sigma_o > \sigma_c$, the electrostatic regime is compressed to such a small region as to render channel tracking totally ineffective. In the other extreme, if $\sigma_o \ll 0.1$ and there is no density channel, the tracking force becomes very weak and linearly proportional to σ_o for the cases of on-axis equilibrium[10]. For cases we have studied, σ_c is around 0.8, and the optimum conductivity for on-axis tracking is around $\sigma_o = 0.1$.

We have not yet included a self-consistent envelope equation in our code, but we can estimate the effect of a trumpet-shaped beam head on tracking by assigning an envelope to the beam radius (normalized to the fully-pinched beam

radius),

$$r_b = 1.0 + \beta\, e^{-\zeta/\alpha}, \tag{6}$$

where we choose $\beta = 10.0$ and $\alpha = 2.0$. We fix $r_c = 1.0$. Consistent with the narrow-channel pencil beam case (Fig. 5), the beam is found to detrack for Y $<<$ 1.0 and track for larger displacements. Figure 10 shows the tracking force in σ, $\sigma + n$ and n channels with Y = 1.5. The strongest force occurs in $\sigma + n$ channel. Channel tracking of a beam with a self consistent envelope will be reported in a later publication.

Figure 11 shows the variation of the n channel force for two cases with Y = 1.5 and on-axis channel density $\rho_g(r = 0) = 0.1$ atm and 0.2 atm. In each case, the density outside the channel is 1 atm. This clearly indicates a deeper density channel gives better off-axis tracking, as might be expected.

The results for the parametric dependence on r_c, Y and types of channel by the tracking force are summarized in Table I for the pencil beam and Table II for the trumpet beam. The last column represents the maximum tracking force normalized to the pinch force.

In Fig. 12, we show the resultant tracking force f_t on a ring of beam electrons located between r and $r + \Delta r$ at a given ζ, for Y = 0.1 and 1.5. A $\sigma + n$ channel is chosen for this example. For both values of Y, the central core of the beam always feels a net force that attracts it toward the channel, even though the net force on the beam slice as a whole is detracking for Y = 0.1. This phenomena has previously been observed in linearized simulation codes using wide channels[10]. However, the portion of the beam that feels an attractive force is very small ($r/r_b < 1/3$) for the Y = 0.1 case. Since the tracking or detracking force is usually 10^{-2} to 10^{-3} times smaller

than local pinch force, which holds the beam slice together, we do not expect the beam to tear itself apart in any gross sense so that its central part tracks and its wings fly apart.

III. Analytic and Model Calculations

The DYNASTY-II code calculations presented in previous sections have arrived at conclusions regarding the beam-channel interaction that were not anticipated and may seem peculiar, namely that if the channel is initially weakly ionized ($4\pi\sigma_o r_b/c \lesssim 0.8$) the beam head is attracted toward the channel axis if the beam is narrow, but is repelled from the channel axis and attracted toward a certain fixed displacement $Y = Y_o$ if the beam is broad. (If the channel is initially unionized, the beam is practically force-free for $Y \lesssim Y_o$, but feels a tracking force when $Y > Y_o$, whether r_b/r_c is large or small.) In this section we shall consider a simple example which can be explored by means of physical arguments and elementary mathematics, and which elucidates the origin of these effects.

We consider a beam of specified charge density profile $\rho_b(\zeta, r)$ and we consider only the limit of small σ, applicable to the head of a beam propagating in neutral gas or in a weakly pre-ionized channel. It is worth mentioning that for an ultrarelativistic beam ($\gamma >> 1$) Maxwell's equations reduce exactly to Lee's field equation (1) in the limit of small σ (as well as the limit of large σ and several other limits)[4]. It has further been pointed out that to first order in σ the forces on the beam due to Eq. (1) reduce to two dimensional electrostatics[11]. We shall reproduce the expansion that leads to this conclusion.

To order σ^o, Eq. (1b) yields

$$\nabla_\perp^2 A^{(o)} = \nabla_\perp^2 \phi^{(o)} + \psi(\underline{r}_\perp), \tag{7}$$

where ψ is some function independent of ζ. Since both A and ϕ are zero ahead of the beam (no precursor signals can get ahead of the beam in the

ultrarelativistic limit), and A and ϕ can be taken to be equal at large radii (either metallic or vacuum boundary conditions at large r), we find

$$A^{(o)} = \phi^{(o)}. \tag{8}$$

From Eq. (1a)

$$\nabla_\perp^2 \phi^{(o)} = - 4\pi \rho_b, \tag{9}$$

i.e.,

$$\phi^{(o)}(r) = 2 \int_r^\infty \frac{dr'}{r'} \int_o^{r'} dr'' 2\pi r'' \rho_b(r''), \tag{10}$$

where ρ_b is the beam charge density. To order σ^o, the beam is force-free: its vacuum electric and magnetic self-forces cancel (in the ultrarelativistic limit).

To next order, Eqs. (1a) and (8) with appropriate boundary conditions yield,

$$A^{(1)} = 0, \tag{11}$$

and Eq. (1b) yields,

$$\nabla_\perp^2 \phi^{(1)} = - 4 \pi \rho^{(1)}, \tag{12}$$

where $\rho^{(1)}$ is the plasma charge density, given by,

$$\frac{\partial \rho^{(1)}}{\partial \zeta} = \frac{1}{c} \nabla_\perp \cdot \sigma \nabla_\perp \phi^{(o)}. \tag{13}$$

Through first order in σ, the force on the beam is entirely due to the electrostatic potential $\phi^{(1)}$, which is specified by the two-dimensional electrostatic field equation (12), with the plasma charge distribution (13) as the only source. Henceforth, we simplify notation by dropping the superscripts on $\phi^{(1)}$ and $\rho^{(1)}$. Equations (7)-(13) have previously been derived by Briggs and Lee[11].

Next we consider the specific case of a pencil beam of Gaussian profile,

$$\rho_b = \rho_{bo} \exp(-r^2/r_b^2), \tag{14}$$

propagating in a specified displaced Gaussian conductivity profile,

$$\sigma = \sigma_o(\zeta)\exp\left[\frac{x^2 + (y + Y)^2}{r_b^2/\alpha}\right] \equiv \sigma_o(\zeta)\exp\left(-\frac{\alpha \breve{r}^2}{r_b^2}\right). \tag{15}$$

Equations (10) and (13) may be integrated in closed form for this case, yielding

$$\rho = -\frac{16\pi^2 \rho_{bo}}{c} \int_o^\zeta d\zeta' \sigma_o(\zeta') \left[\left(1 + \alpha + \frac{\alpha y Y}{r^2}\right)\exp\left(-\frac{r^2 + \alpha \breve{r}^2}{r_b^2}\right)\right.$$

$$\left. - \alpha\left(1 + \frac{Yy}{r^2}\right) \exp\left(-\frac{\alpha \breve{r}^2}{r_b^2}\right)\right]. \tag{16}$$

We could solve Poisson's equation (12) and calculate the resultant force on the beam for any Y, but this could only be carried out numerically and would not be particularly illuminating. We therefore follow the alternative course

of examining separately the limits of small Y and large Y.

If $Y \ll r_b$ and we linearize in Y, Eq. (16) may be written as the sum of a term symmetric about the conductivity channel axis and another term symmetric about the beam axis,

$$\rho(\underset{\sim}{r}_\perp) = \rho_1(\check{r};\alpha) + \rho_2(r;\alpha), \tag{17}$$

where $\check{r}$ is the distance from channel axis,

$$\rho_1(r;\alpha) = -\alpha\, 16\pi^2\rho_{bo} \int_o^\zeta d\zeta' \sigma(\zeta') \left\{ -\exp\left(-\frac{\alpha\check{r}^2}{r_b^2}\right) \right.$$

$$\left. + \exp\left[\frac{(1+\alpha)\check{r}^2}{r_b^2}\right] + \frac{1}{2}\,\mathrm{Ei}\left(\frac{\alpha\check{r}^2}{r_b^2}\right) - \frac{1}{2}\,\mathrm{Ei}\left[\frac{(1+\alpha)\check{r}^2}{r_b^2}\right] \right\}, \tag{18}$$

and

$$\rho_2(r;\alpha) = -16\pi^2\rho_{bo} \int_o^\zeta d\zeta' \sigma(\zeta') \exp\left[\frac{(1+\alpha)r^2}{r_b^2}\right]$$

$$- \frac{\alpha}{2}\,\mathrm{Ei}\left(\frac{\alpha r^2}{r_b^2}\right) + \frac{\alpha}{2}\,\mathrm{Ei}\left[\frac{(1+\alpha)\check{r}^2}{r_b^2}\right], \tag{19}$$

where $\mathrm{Ei}(x) \equiv -\int_{-x}^{\infty} dt\, t^{-1} e^{-t}$ is the exponential integral. Because of axisymmetry, fields derived from $\rho_2(r)$ exert no resultant force on the beam, and thus the resultant force on any given beam slice, to first order in Y (or the total potential of a beam slice to second order in Y) derives entirely from $\rho_1(\check{r})$. Since ρ_1 is itself axisymmetric as a function of $\check{r}$, the potential associated with the charge distribution ρ_1 is immediately specified to be

$$\phi_1(\check{r};\,\alpha) = -\int_o^{\check{r}} \frac{d\check{r}'}{\check{r}'} \int_o^{\check{r}'} d\check{r}''\, 4\pi \check{r}''\, \rho_1(\check{r}''). \tag{20}$$

We note from Eq. (18) the following properties of ρ_1:

$$\rho_{bo}\, \rho_1(\check{r}) < 0 \qquad \text{for } 0 < \check{r} < \check{r}_o, \tag{21a}$$

$$\rho_{bo}\, \rho_1(\check{r}) > 0 \qquad \text{for } \check{r}_o < \check{r} < \infty\ , \tag{21b}$$

$$\rho_{bo} \int_o^{\infty} d\check{r}\ 2\pi \check{r}\, \rho_1(\check{r}) = 4\pi \rho_{bo}^2 \int_o^{\zeta} d\zeta'\, \sigma(\zeta') > 0, \tag{21c}$$

where $\check{r}_o/r_b$ is a function of α determined by the equation,

$$\exp(-\alpha \check{r}_o^2/r_b^2) - \tfrac{1}{2}\, \mathrm{Ei}(\alpha\, \check{r}_o^2/r_b^2) = \exp[-(1+\alpha)\check{r}_o^2/r_b^2] - \tfrac{1}{2}\, \mathrm{Ei}[(1+\alpha) r_o^2/r_b^2]. \tag{21d}$$

Properties (21a) and (21b) might well be expected, since (for an electron beam, with $\rho_{bo} < 0$) a positive image charge collects in the region of highest conductivity, leaving a negative plasma charge elsewhere. Equation (21c) may be a bit surprising, since the plasma must be globally neutral; however it is another manifestation of image charge formation: the component ρ_1 has negative total charge, while the component ρ_2, which is closer to the beam but which exerts no resultant force on the beam, has positive total charge. These properties may reasonably be expected to hold generally for a beam with any monotonic profile $\rho_b(r)$ in a channel $\sigma(\check{r})$ of monotonic profile.

We consider the forces on a beam slice displaced from the axis of the central potential $\phi_1(\check{r})$ of Eq. (20). We shall consider the beam slice to be a

rigid object, made up by fixed point "elements" of charge density $\rho_b(\underset{\sim}{r}_\perp)$, or of fixed rings of charge density at radius r. The force on a ring is the resultant of the forces on its elements; the force on the whole beam slice is the resultant of the forces on its rings. No account is taken here of the fact that the beam is made up of moving electrons that are not confined to any particular ring, or that the beam may tend to distort from its circular shape, or even tear apart, because the channel force is different on different parts of the beam. In other words, we are only calculating the forces on the beam here, not following the beam dynamics at all.

Using the channel-centered coordinate system $\breve{r}$, we define the potential energy of a rigid uniform ring of radius R with its center displaced by Y from the origin, as

$$\Phi_r(R,\ Y;\ \alpha) = \rho_b(R) \iint d\underset{\sim}{r}_\perp\ \delta(|\underset{\sim}{\breve{r}} + \underset{\sim}{Y}| - R)\ \phi_1(\breve{r},\ \alpha), \tag{22}$$

and the potential energy of the entire beam slice, also displaced by Y, as

$$\Phi_s(Y,\alpha) = \int_0^\infty dR\ 2\pi R\ \Phi_r(R,Y,\alpha). \tag{23}$$

To simplify notation, we assume that $Y > 0$. We now proceed through a series of physical arguments that specify the sources and the sign of the force on beam elements, rings, and on the beam slice. Although we have used an expansion in small Y to derive the separation of the plasma charge into ρ_1 and ρ_2, Eq. (11), we do not need to invoke the smallness of Y in some of these arguments.

(i) The part of $\rho_1(\breve{r})$ with $\breve{r} > \breve{r}_1$ exerts no net force on a beam element at location $\underset{\sim}{\breve{r}}_1$. This is apparent from Eq. (14).

(ii) It follows that a ring of plasma charge with radius $\breve{r}$ exerts no net force on a ring of beam charge with radius R if $\breve{r} > R + Y$, since the beam ring is completely contained within the plasma ring.

(iii) It is also true that an element of plasma charge exerts no net force on a ring of beam charge with radius R if it is contained within the ring. This follows because, from (i) the beam ring exerts no force on the plasma element and according to Newton's third law, the reverse is true as well.

(iv) It follows from (ii) and (iii) that if $R > Y$, the force on the beam ring of radius R is determined only by the plasma charge within the crescent shaped region between $r = R$ and $\breve{r} = R + y$, as shown in Fig. 13. (We recall that r is the beam-centered coordinate, $r = |\breve{r} - Y|$.) It is obvious then that the electron beam ring is attracted back toward $Y = 0$, if the plasma charge $\rho_1(\breve{r})$ is positive throughout $R - Y \leq \breve{r} \leq R + Y$, and that the beam ring is pushed toward larger displacement Y if $\rho_1(\breve{r})$ is negative throughout $R - Y \leq \breve{r} \leq R + Y$, i.e., that $\partial\Phi_r/\partial Y$ is positive in the former case, and negative in the latter. If, in particular, Y is infinitesimal, then the sign of the force $\partial\Phi_r/\partial Y$ is determined entirely by the sign of $\rho_1(R)$. When we note the properties (15a) and (15b) of $\rho_1(r)$, it is apparent that $\partial\Phi_r/\partial Y$ is positive for $R < \breve{r}_o$ and negative for $R > \breve{r}_o$, i.e. the inner portions of the beam are attracted toward the channel and the outer portions repelled, if the displacement Y is small[10].

Next we consider the force $\partial\Phi_s/\partial Y$ on the entire beam slice, for the case of a small displacement Y of the beam from the channel. According to (22) and (23),

$$\Phi_s(Y,\alpha) = \int_o^\infty dR\ R\ \rho_b(R) \int_o^{2\pi} d\theta\ \Phi_1(\breve{r} = R + Y \sin\theta). \qquad (24)$$

Expanding to order Y^2 and using Eq. (14) this becomes

$$\Phi_s(Y, \alpha) \approx \Phi_s(0, \alpha) - Y^2\, 2\pi^2 \int_0^\infty dR\, R\, \rho_b(r = R)\, \rho_l\, (\tilde{r} = R). \qquad (25)$$

The beam slice is attracted toward the channel if the integral in (25) is negative, or repelled if it is positive.

If the slice is narrow, i.e., $\alpha \ll 1$ and ρ_b falls off much faster than ρ_l, the integral is determined entirely by $\rho_l(\tilde{r} < \tilde{r}_o)$ and, according to (21a), is negative. The slice is attracted toward the channel, since it is made up entirely of narrow rings which, we have seen, are attracted toward the channel. In the opposite limit of a broad beam, the $\rho_b(R)$ can be approximated by $\rho_b(0)$ in the integral, and then the integral is positive, according to (21c). In this case the central part of the beam is attracted toward the channel and the outer part repelled, but the latter dominates. The transition between a narrow beam with $\partial^2\Phi_s(Y = 0, \alpha)/\partial Y^2 > 0$ and a broad beam with $\partial^2\Phi_s(Y = 0, \alpha)/\partial Y^2 < 0$ occurs for the value α_o of α defined by

$$\int_0^\infty dR\, R\, \rho_b(R)\, \rho_l(R) = 0. \qquad (26)$$

Using Eqs. (14) and (18) for ρ_b and ρ_l, we find after some algebra that α_o is defined as the solution of the equation

$$(1 + \alpha_o)\, (2 + \alpha_o) = 2\, \ln[\alpha_o(2 + \alpha_o)(1 + \alpha_o)^{-2}]. \qquad (27)$$

Next we consider the limit of a beam that is wholly outside the channel, i.e. $Y \gg r_b$ and $Y \gg \alpha^{-1/2} r_b$. In this case, it is clear from two-dimensional

electrostatics that the beam will polarize the channel, leading to an attractive force between beam and channel that is proportional to Y^{-3}. This holds whether the beam is narrow or broad compared to the conductivity channel. We have already seen that in the other limit $Y \to 0$, the beam channel force is attractive for a narrow beam ($\alpha \ll 1$) and repulsive for a broad beam ($\alpha \gg 1$). Thus, we can sketch the potential $\Phi_s(Y; \alpha)$. This is done in Fig. 14. If the beam is narrow (Fig. 14a), the equilibrium of the beam is on-axis in the channel, but if the beam is broad (14b), the equilibrium position of the beam is displaced from the channel axis by some quantity Y_o, where Y_o/r_b is a function of α.

IV. Conclusions

In this report, we have studied in some depth the conditions in which a beam can track a preformed channel. The results can be summarized as follows:

(a) As long as the initial channel conductivity $\sigma_o (= 4\pi\sigma r_b/c)$ is less than 0.8, the beam always tracks the channel, in the sense that the head of the beam is attracted to an equilibrium position that is either on the channel axis or off-axis in the channel by a specified displacement that is typically of the order of the beam radius.

(b) For a pure density channel, the equilibrium is always off-axis. For other types of channels, the equilibrium position of each beam slice is at the channel axis or off-axis depends on the ratio of channel radius to beam radius, r_b/r_c. For a pencil beam, the equilibrium is off axis if $r_b/r_c > 1.0$. This may mean that the equilibrium is typically off axis for a self-consistent modeled beam with an expanded head. If $r_b/r_c < 1.0$ for a pencil beam, the equilibrium is on axis.

(c) A pure conductivity channel ($\sigma_o \sim 0.1$) gives the best on-axis tracking. A combination of conductivity and density channel gives the strongest off-axis tracking.

(d) The central part of the beam always feels a net force attracting it to the channel, even when the average force on the whole beam slice is detracking. But for this case, the portion that feels a tracking force is usually a small part of the beam slice. Since the tracking force is usually at least 10^{-2} times smaller than the local pinch force, which holds the slice together, we do not expect the beam to tear itself apart with the central part tracking the channel and the outer part expelled from the channel. Our model is not yet adequate

to test this supposition, however. (Nor are linearized particle simulation codes adequate for this purpose.)

(e) The ratio of the tracking force to pinch force at full current (F_t/F_p) is about 10^{-5}. The angle of deflection due to channel tracking is therefore very small. We can estimate its magnitude as

$$\theta \sim (I/I_A\gamma)^{1/2}(F_t/F_p)^{1/2}. \tag{28}$$

For typical laboratory experiments, this tracking force is too small to be detected. For example, an NRL experiment was performed with an 8 kA, 1 MeV beam with radius 0.75 cm, propagated into a reduced density channel with $p_g = 0.25$ atm on axis and very little residual conductivity[8]. No appreciable movement of the beam centroid was detected after one meter of propagation, in agreement with Eq. (28) which gives a deflection angle $\theta \sim 1.5\times10^{-3}$ radians, too small to be measured. In a more recent experiment, the same beam was propagated in a reduced density ammonia channel with on-axis density 10 torr and background density 40 torr. It was found that the beam body hosed violently, and no tracking was detected.

Acknowledgments

We are grateful to J. R. Greig, R. Hubbard, G. Joyce, D. Murphy, and W. Sharp for helpful discussions. The work was sponsored by the Defense Advanced Research Projects Agency (DOD) under ARPA Order No. 4395, Amendment No. 9, and monitored by the Naval Surface Weapons Center.

Table I - Pencil Beam

r_c/r_b	Channel	Y/r_b	$(F_t/F_p)_{max}$
2.0	σ	0.1	1.4×10^{-6}
2.0	$\sigma + n$	0.1	1.2×10^{-6}
2.0	n	0.1	-
2.0	σ	1.5	8.1×10^{-5}
2.0	$\sigma + n$	1.5	1.1×10^{-4}
2.0	n	1.5	1.1×10^{-5}
1.0	σ	0.1	-
1.0	$\sigma + n$	0.1	-
1.0	n	0.1	-
1.0	σ	1.5	2.9×10^{-5}
1.0	$\sigma + n$	1.5	5.3×10^{-5}
1.0	n	1.5	4.6×10^{-5}
0.5	σ	0.1	-
0.5	$\sigma + n$	0.1	-
0.5	n	0.1	-
0.5	σ	1.5	1.8×10^{-5}
0.5	$\sigma + n$	1.5	1.8×10^{-5}
0.5	n	1.5	2.4×10^{-5}

Table II - Trumpet Beam

r_c/r_b	Channel	Y/r_b	$(F_t/F_p)_{max}$
1.0	σ	0.1	-
1.0	$\sigma + n$	0.1	-
1.0	n	0.1	-
1.0	σ	1.5	2.9×10^{-5}
1.0	$\sigma + n$	1.5	6.0×10^{-5}
1.0	n	1.5	3.3×10^{-5}

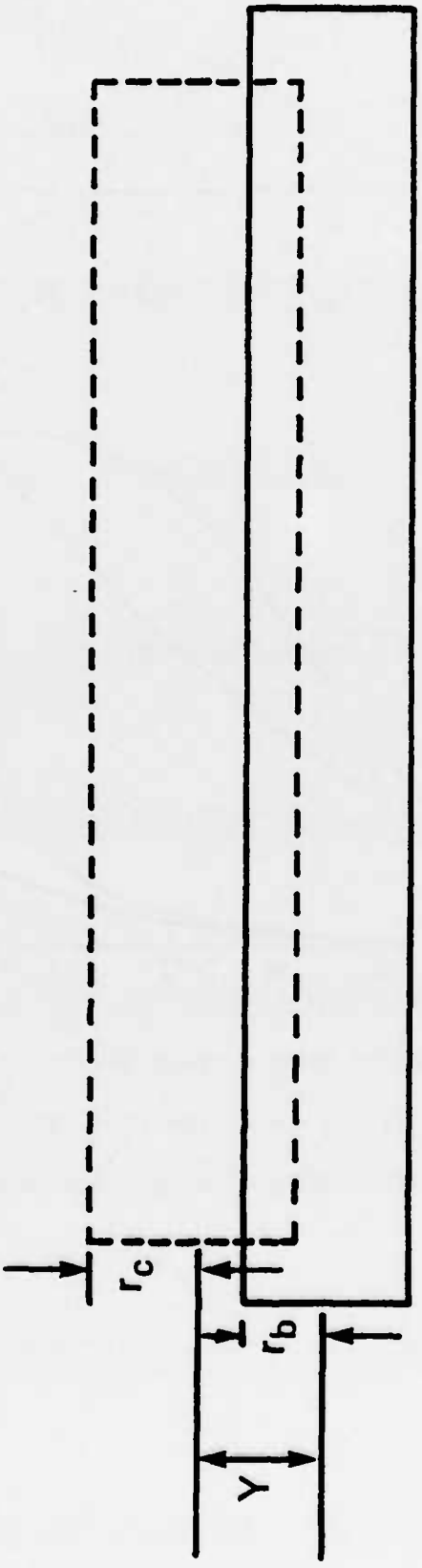

Fig. 1 Relative position of beam to channel.

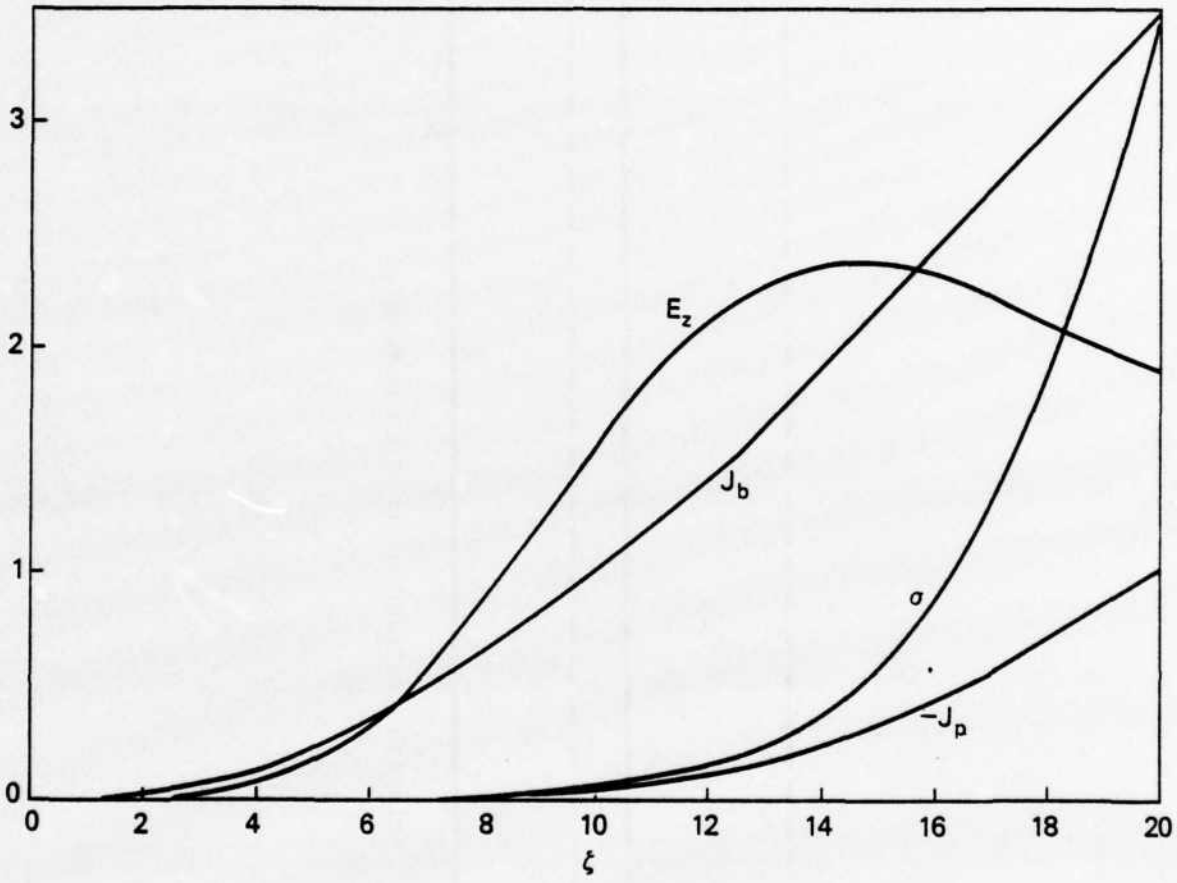

Fig. 2 Typical ζ-dependences of beam current density J_b on the beam axis, plasma current density J_p, axial electric field E_z and conductivity σ on the channel axis near the beam head.

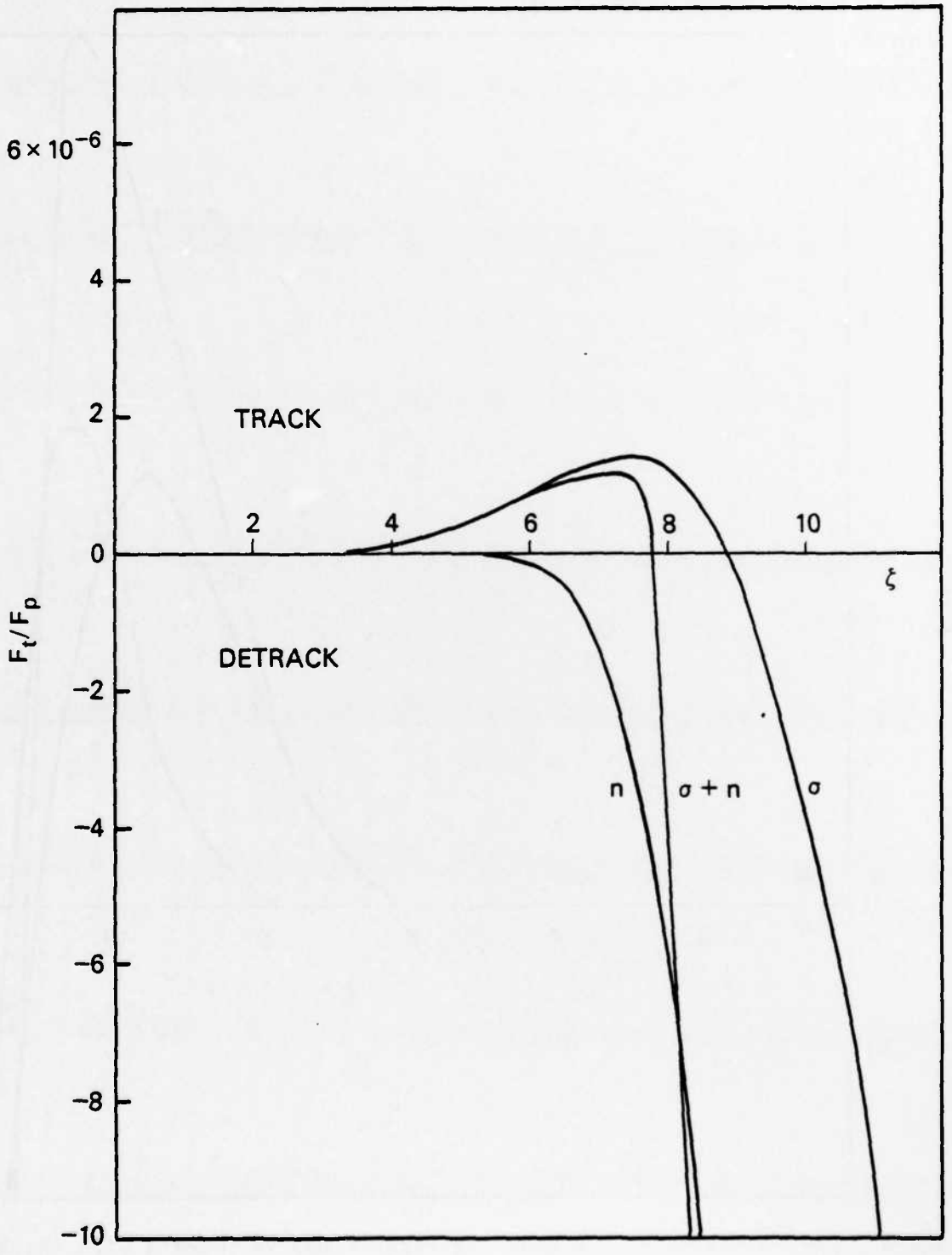

Fig. 3 The variation of the tracking force $F_t(\zeta)$ vs ζ for a wide channel (r_c = 2.0) and a small beam displacement (Y = 0.1).

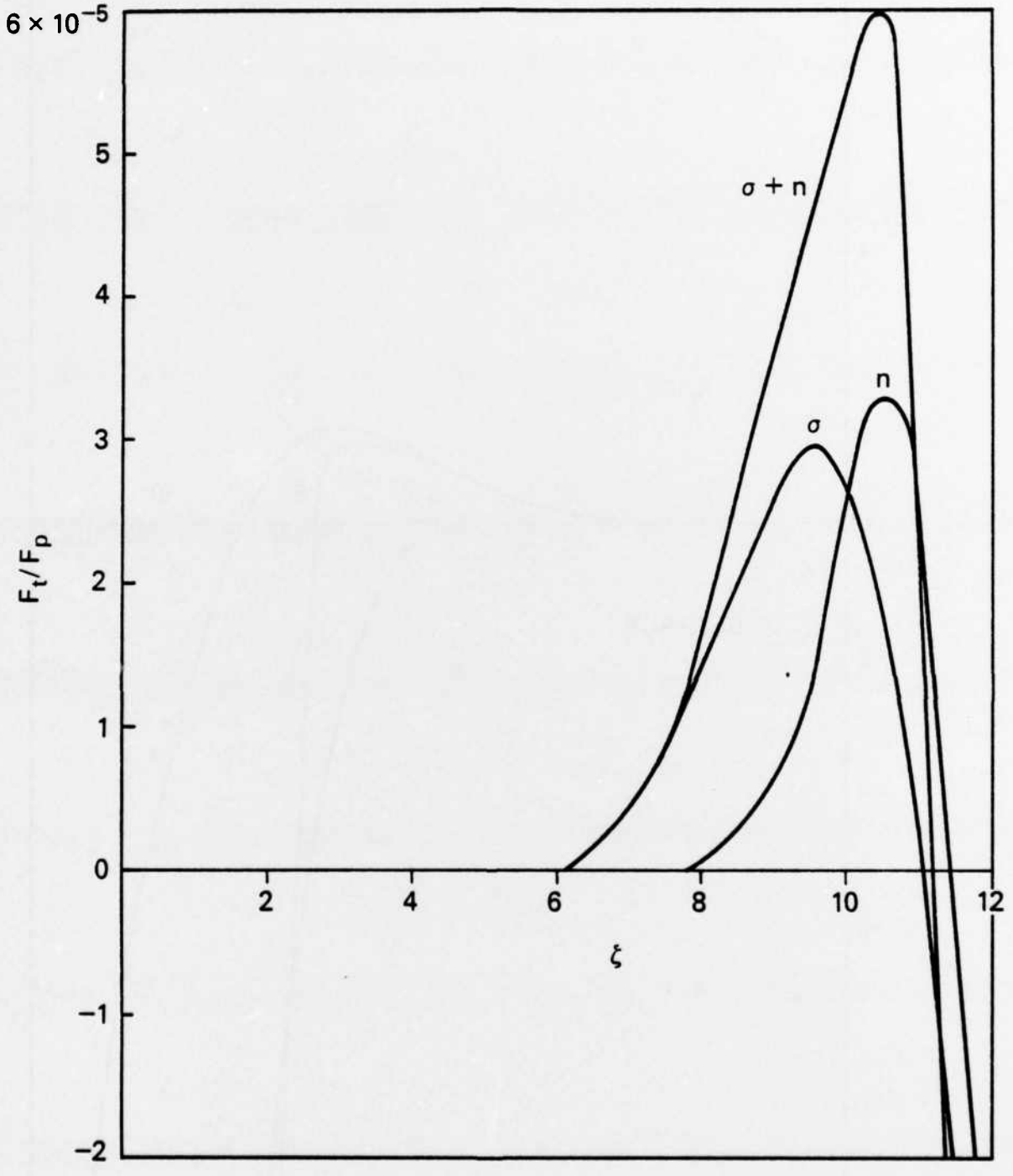

Fig. 4 The variation of the tracking force $F_t(\zeta)$ vs ζ for a wide channel (r_c = 2.0) and a large beam displacement (Y = 1.5).

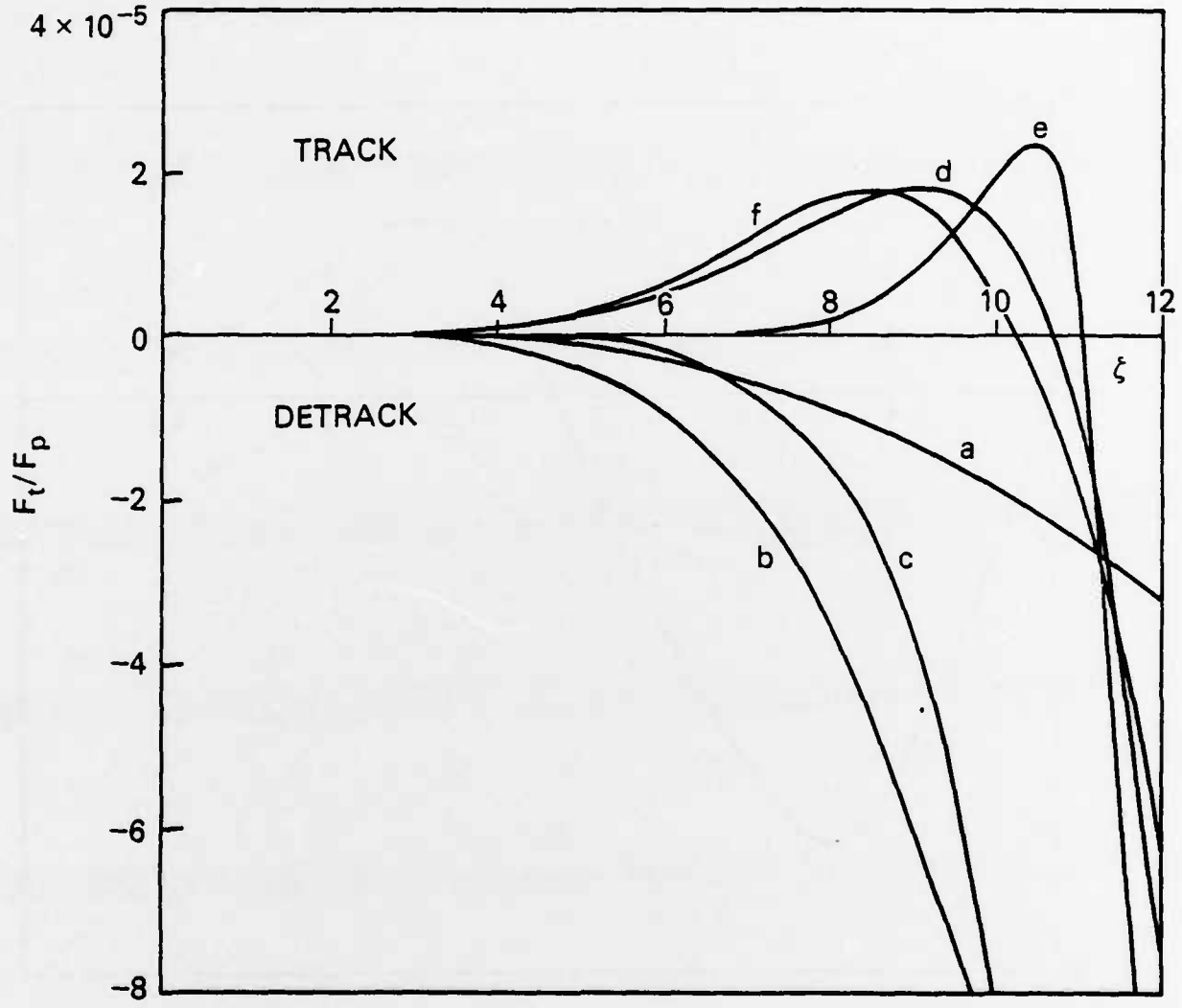

Fig. 5 The dependence of the tracking force $F_t(\zeta)$ on various beam displacements Y for a narrow channel (r_c = 0.5). Curves (a-d) are for σ + n channel. Curve (a) is for Y = 0.1, curve (b) is for Y = 0.5, curve (c) is for Y = 1.0 and curve (d) is for Y = 1.5. Curve (e) is for the n channel with Y = 1.5 and curve (f) is for the σ channel with Y = 1.5.

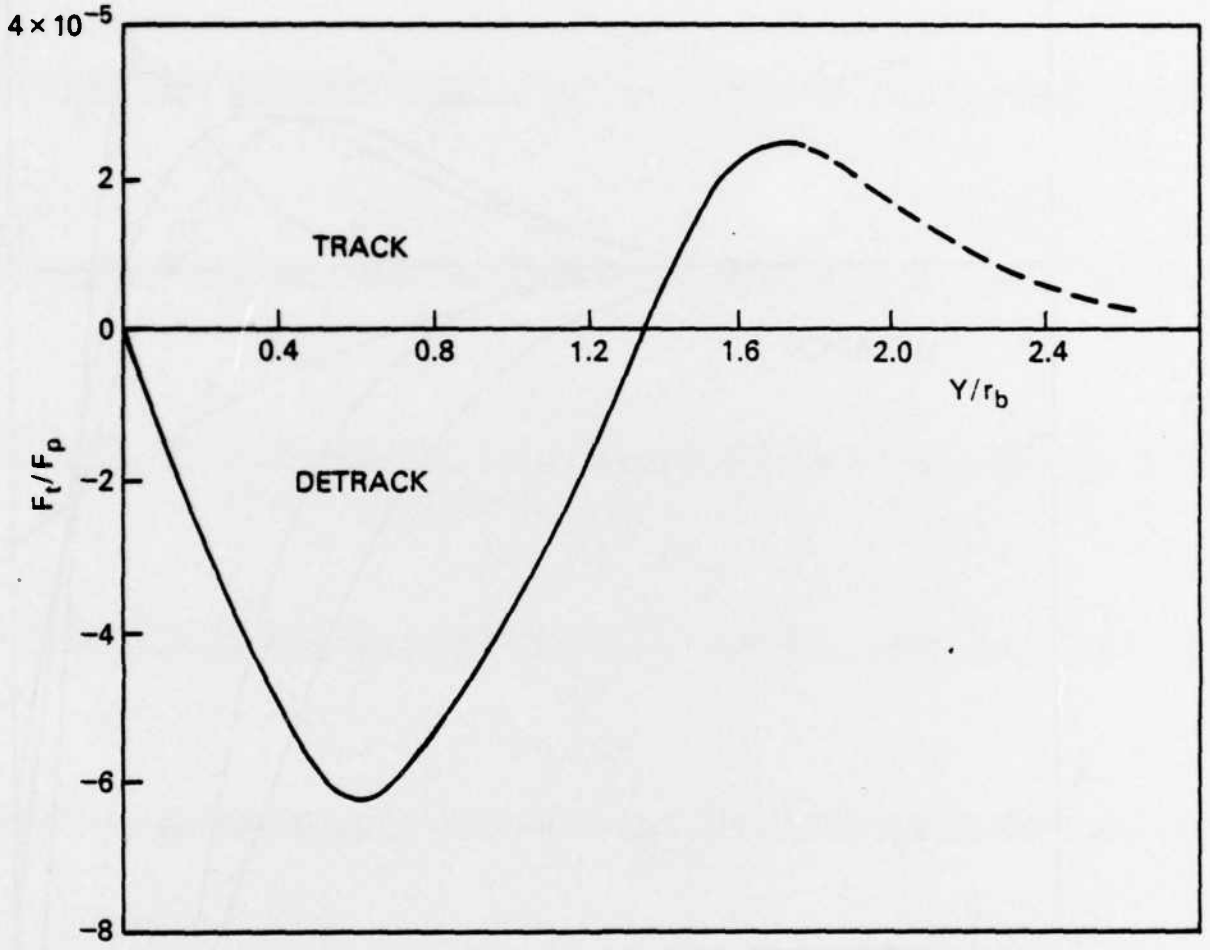

Fig. 6 The dependence of the tracking force as a function of beam displacement Y for $r_c = 0.5$ and $\zeta = 9.0$. Channel type is σ + n.

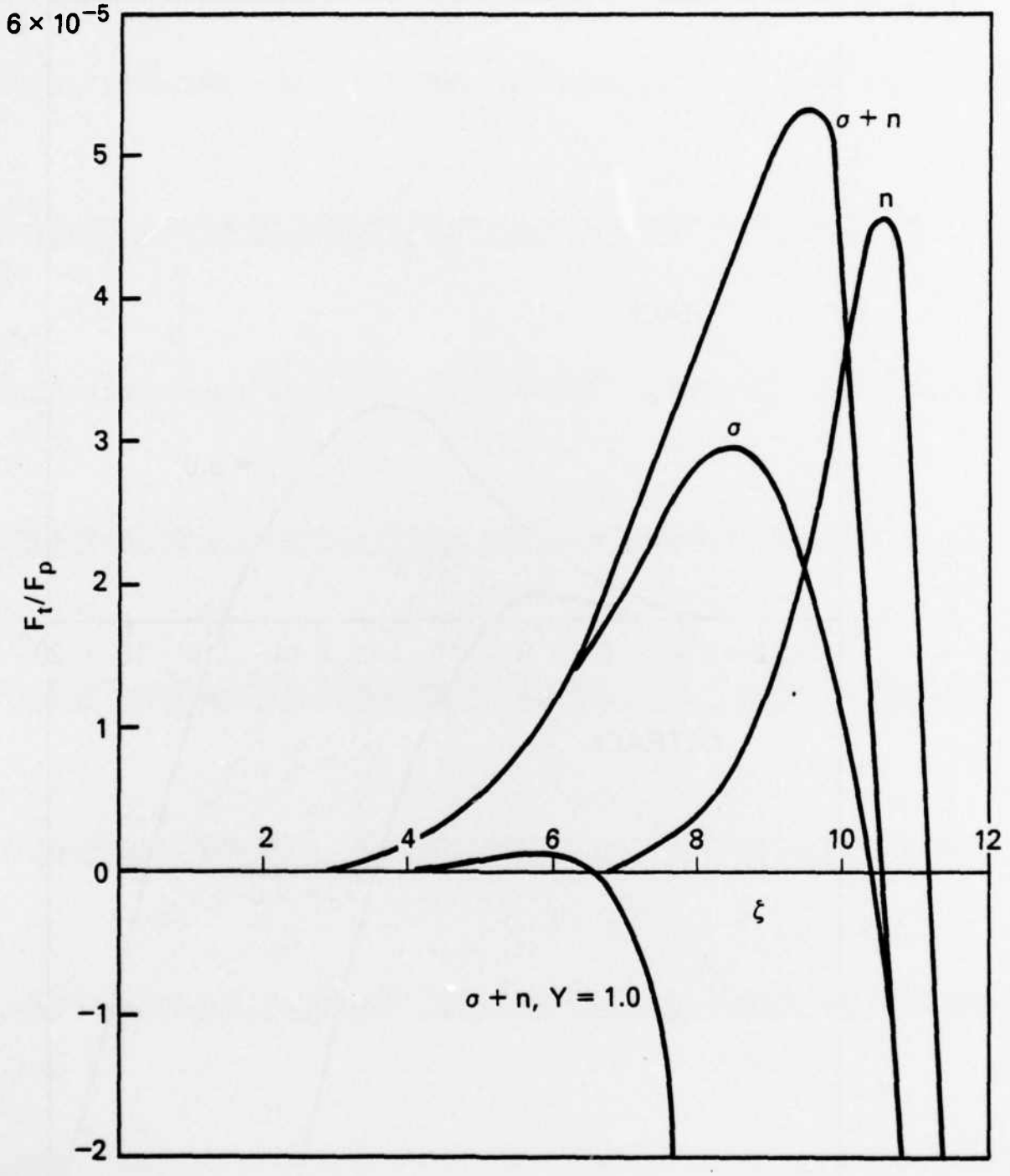

Fig. 7 The variation of the tracking force $F_t(\zeta)$ vs ζ for $r_c = 1.0$ and $Y = 1.5$. The tracking force for $Y = 1.0$ in $\sigma + n$ channel is also shown for comparison.

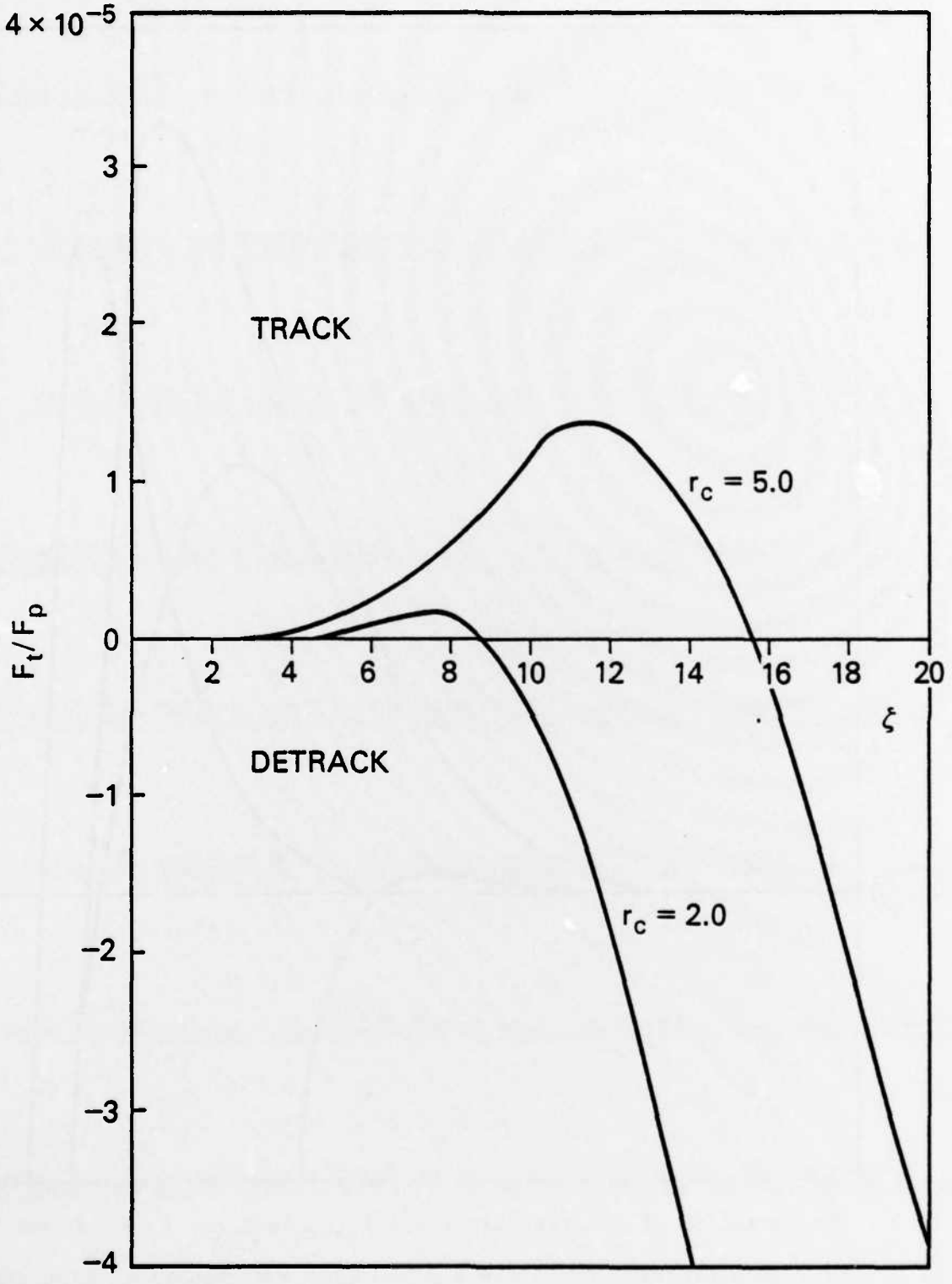

Fig. 8 The tracking forces for two values of channel radius $r_c = 2.0$ and $r_c = 5.0$ are compared. The beam displacement Y = 0.1.

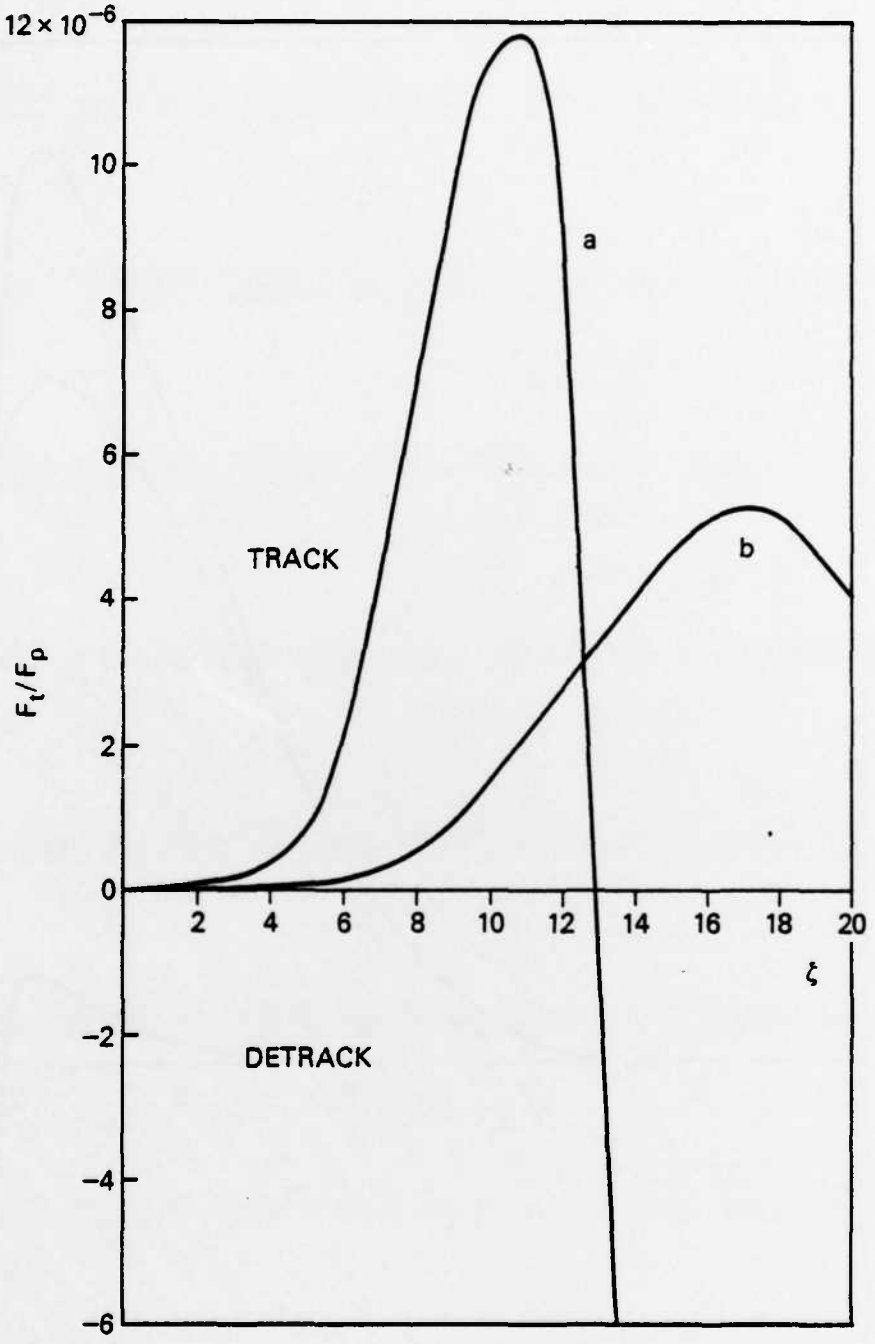

Fig. 9 The dependence of the tracking force on rise time (measured in units of ζ). Curve (a) denotes $\zeta_r = 30$ and curve (b) denotes $\zeta_r = 60$.

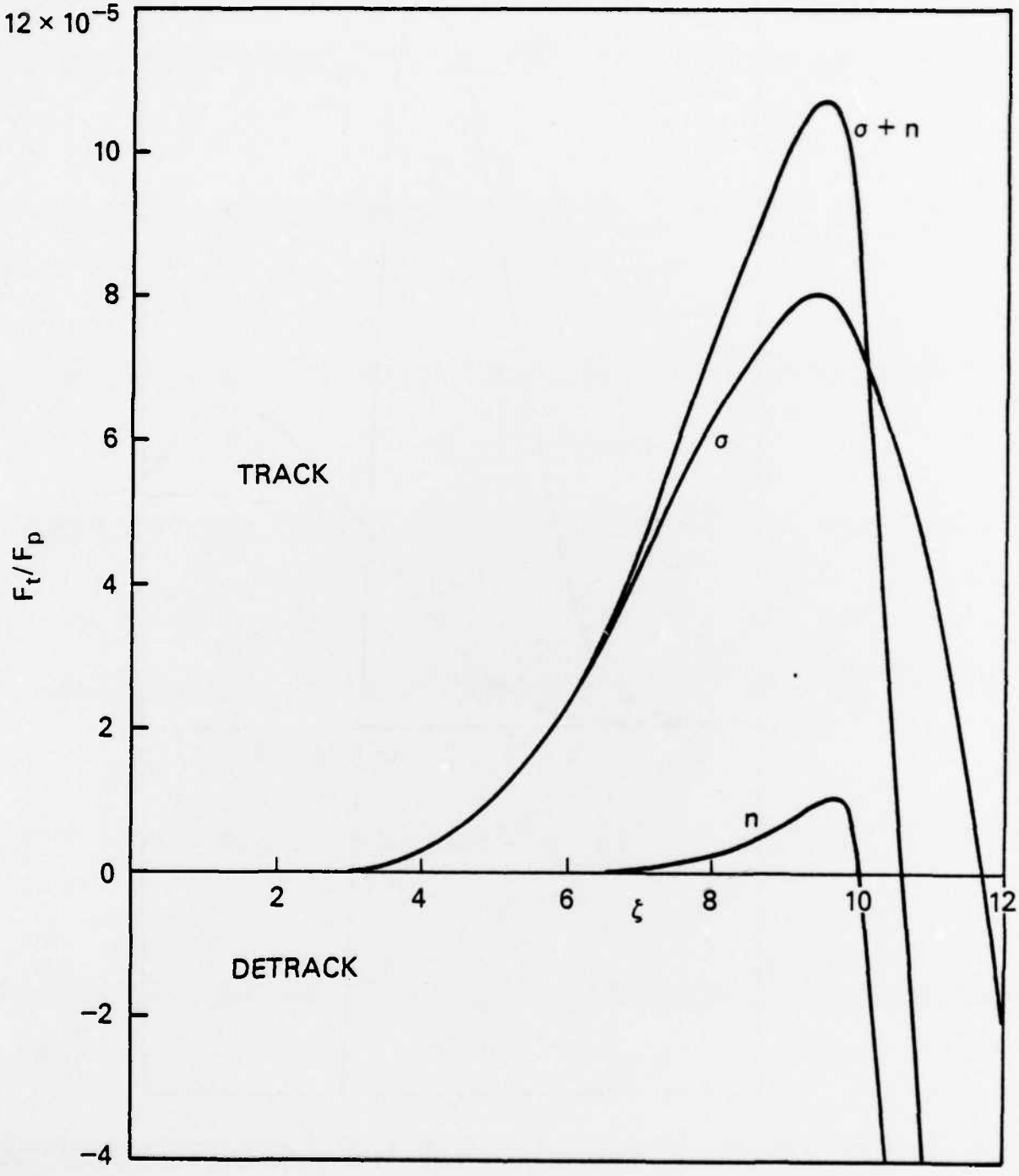

Fig. 10 The dependence of the tracking force F_t of a trumpet beam on three types of channels as a function of ζ, Y = 1.5.

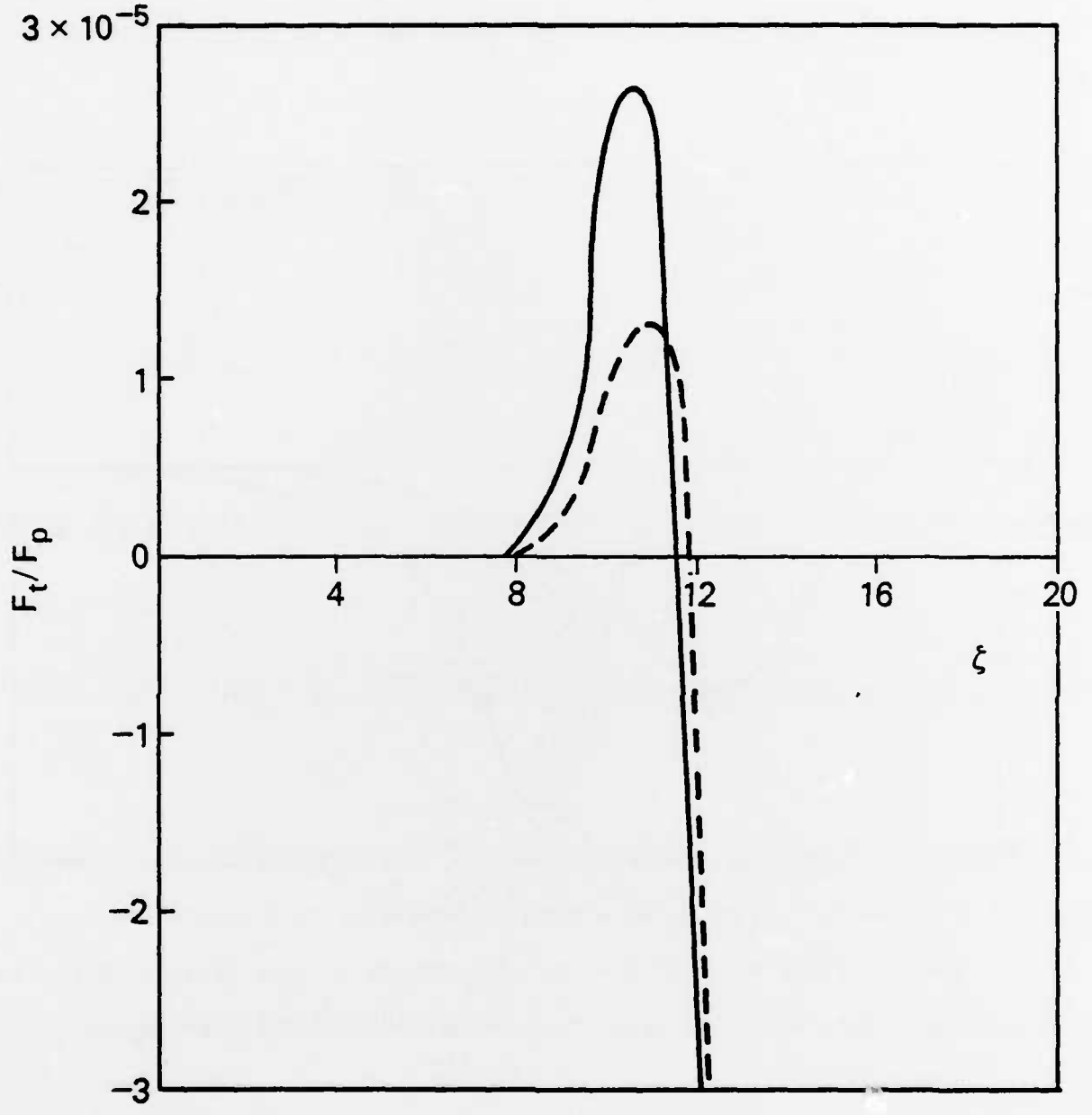

Fig. 11 The dependence of the tracking force on the on-axis channel density with Y = 1.5 for a density channel. Solid curve denotes ρ_g = 0.1 atm and dashed curve denotes ρ_g = 0.2 atm.

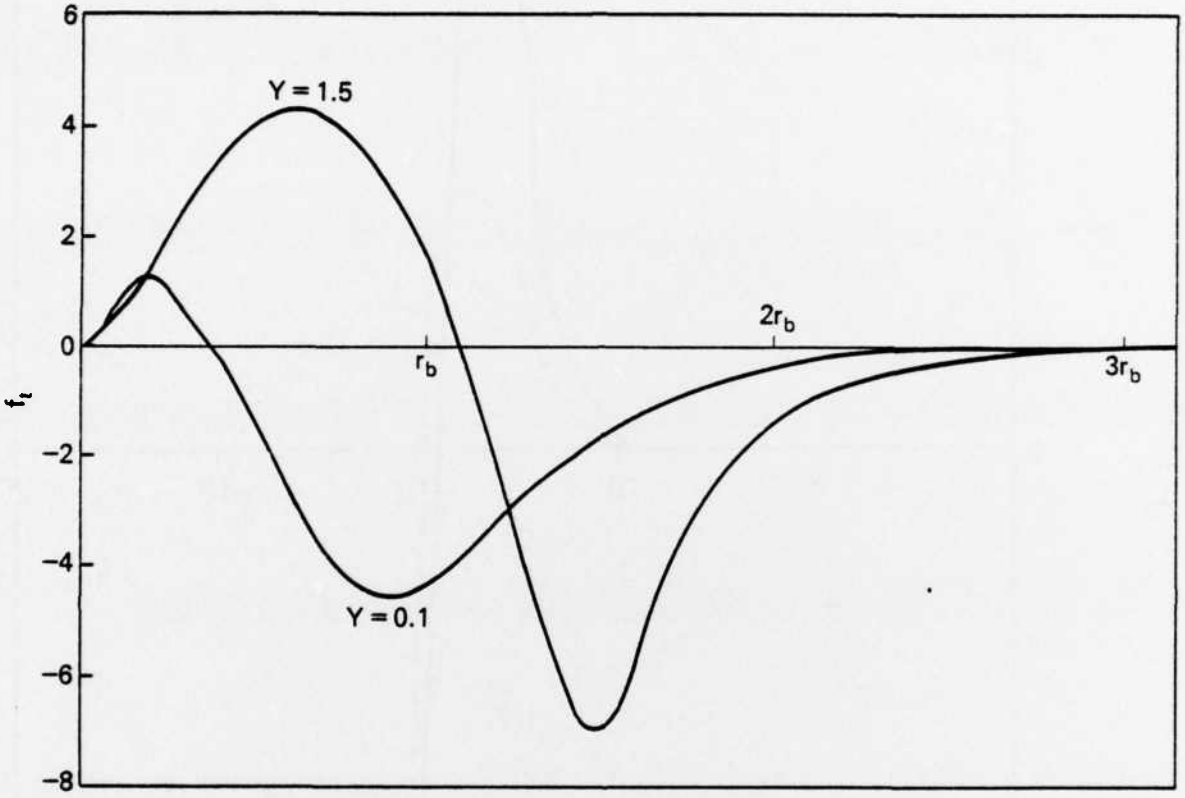

Fig. 12 The tracking force f_t on a ring of beam electrons located between r and r + Δr as a function of r. Two values of beam displacements are plotted, Y = 0.1 and 0.5. The central part of the beam always tracks.

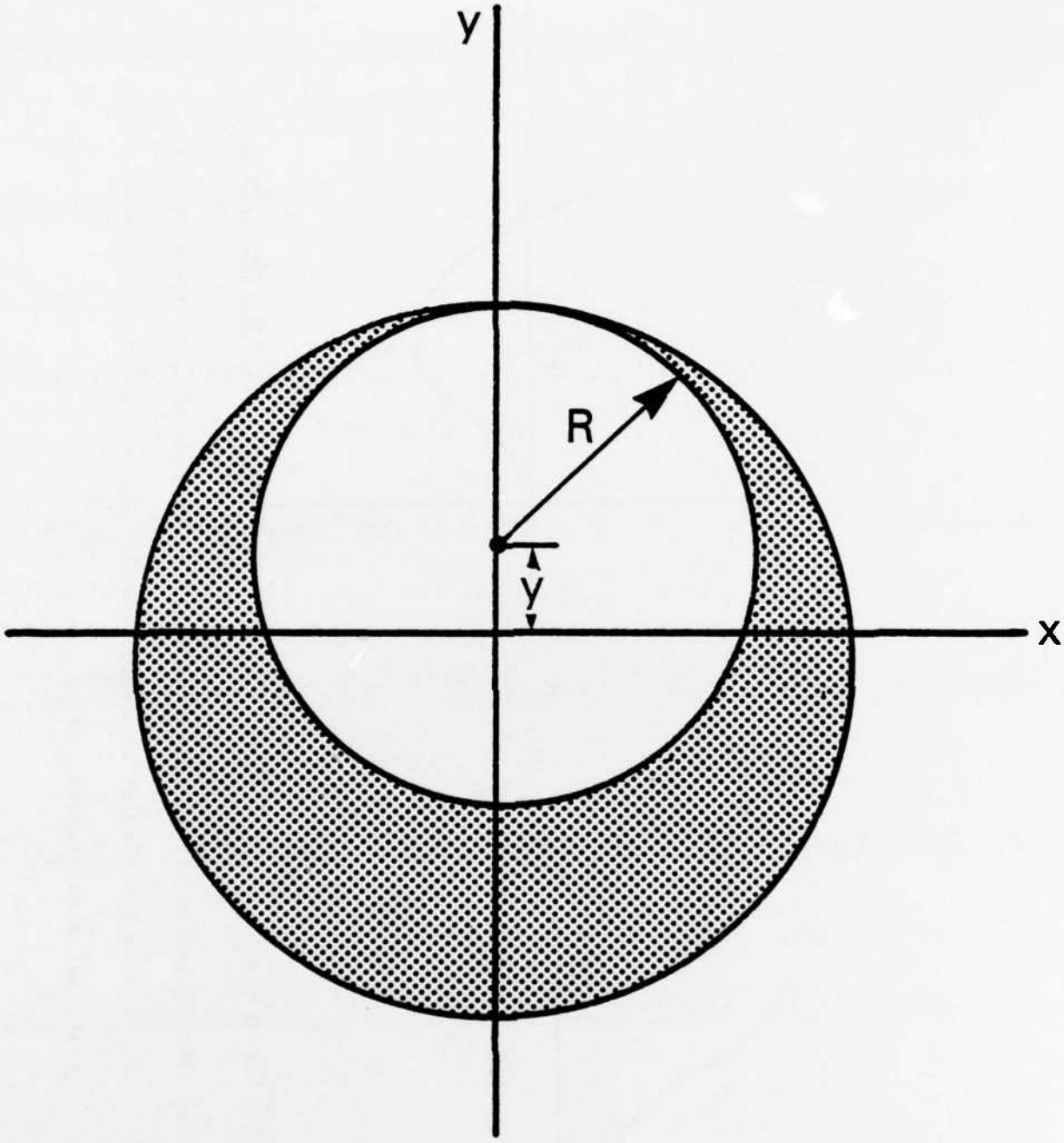

Fig. 13 The force on the beam ring of radius R is due entirely to the plasma charge located in the shaded region.

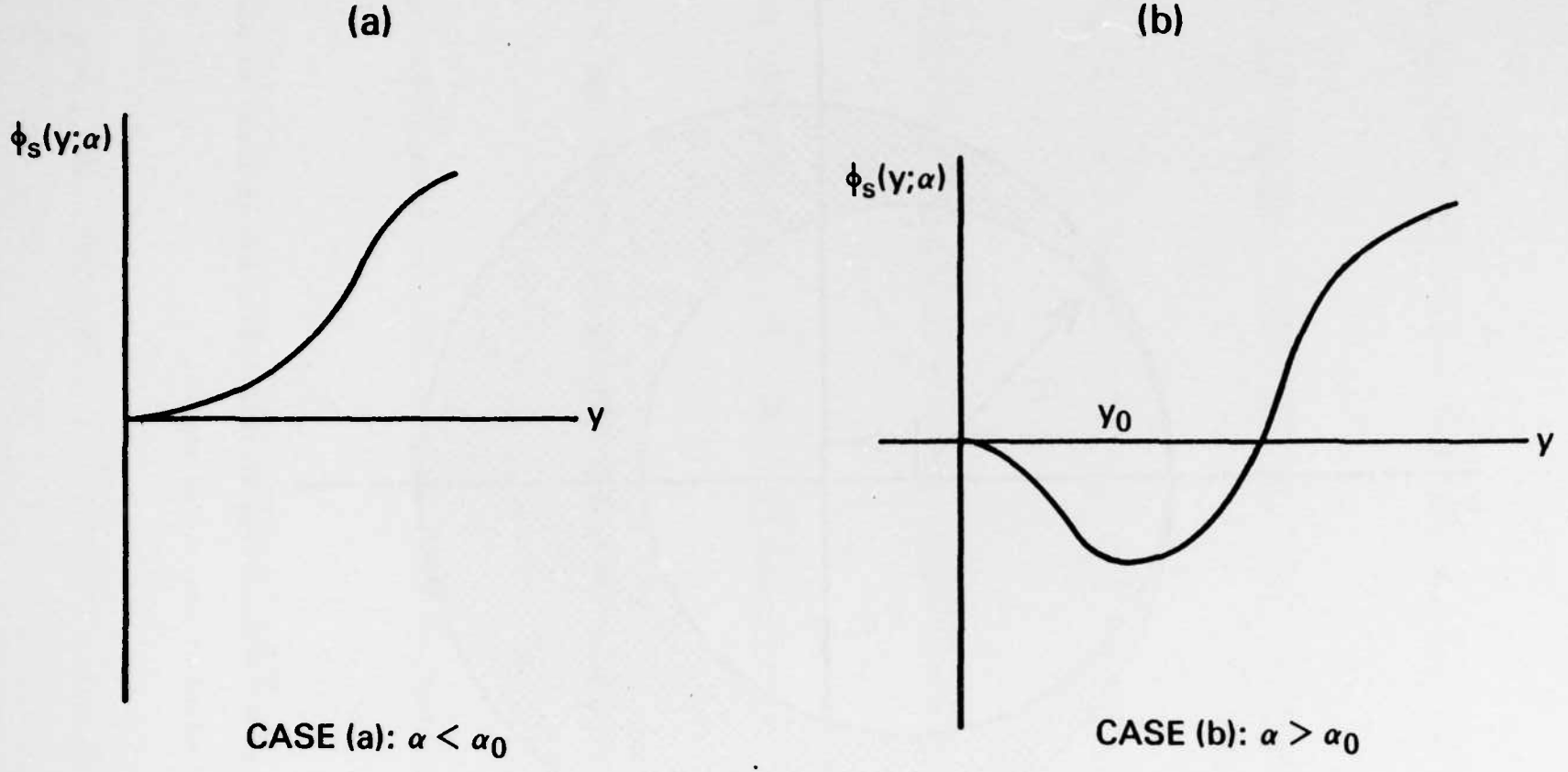

Fig. 14 The variation of the potential ϕ_s as a function of beam displacement Y. Two types of solution exist depending on the ratio (α) of the beam radius to channel radius.

References

1. E. P. Lee, "Model of Beam Head Erosion", Lawrence Livermore National Laboratory, UCID 18768 (1980); W. M. Sharp and M. Lampe, Phys. Fluids 23, 2383 (1980).
2. E. P. Lee, Phys. Fluids 21, 1327 (1978); W. M. Sharp, M. Lampe and H. S. Uhm, Phys. Fluids 25, 1456 (1982); M. Lampe, W. Sharp and R. Hubbard, "Plasma Current and Conductivity Effects in Hose Instability", NRL Memo Report No. 5140 (1983).
3. B. Hui and M. Lampe, NRL Memo Report 5138 (1983) (ADA 131 592); to be published in J. Comp. Physics.
4. E. P. Lee, "The New Field Equations", Lawrence Livermore National Laboratory, UCID-17826 (1976).
5. G. Joyce and M. Lampe, "Numerical Simulation of the Axisymmetric Hollowing Instability", NRL Memo Report 5053 (1983) (AD A 126 937); Phys. Fluids (in press).
6. E. P. Lee, F. W. Chambers, L. L. Lodestro, and S. S. Yu, "Stable Propagation of an Electron Beam in Gas", Proc. of the Second Int. Conf. on High Power Electron and Ion Beam Research and Technology, Cornell Univ., (1977), p. 381; R. F. Hubbard, M. Lampe, S. Slinker, and G. Joyce, Proc. of the Tenth Conf. on Numerical Simulation of Plasmas, San Diego (1983); "VIPER I - A Multi-Component Hose Dynamics Code", JAYCOR Tech. Rpt. J207-81-005 (1981); F. W. Chambers, J. A. Masamitsu, and E. P. Lee, "Mathematical Models and Illustrative Results For the Ringbearer II Monopole/Dipole Beam-Propagation Code", Lawrence Livermore National Laboratory, UCID-19494 (1982).
7. G. Joyce and M. Lampe, Proc. of the Tenth Conf. on Numerical Simulation of Plasmas, San Diego (1983).

8. M. Raleigh, J. D. Sethian, L. Allen, J. R. Greig, R. B. Fiorito, and R. F. Fernsler, "Experiments On the Injection of Relativistic Electron Beams Into Preformed Channels In the Atmosphere, A Feasibility Study", Naval Research Laboratory Memo Report No. 4220 (1980). (AD-A086 732)

9. D. P. Murphy, M. Raleigh, R. E. Pechacek, and J. R. Greig, "Stability of Relativistic Electron Beams in Density Channels - II", Fifth Int. Conf. on High Power Particle Beams, San Francisco, CA, Sep 1983.

10. J. A. Masamitsu, S. S. Yu, and F. W. Chambers, "Beam-Tracking Studies With Ringbearer II", Lawrence Livermore National Laboratory, UCID-19771 (1982).

11. E. P. Lee, "Calculation of a Tracking Force", Lawrence Livermore National Laboratory, UCID-19674 (1983); R. J. Briggs, private communication.